

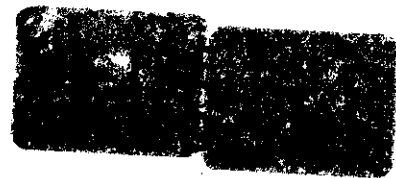
60-07-07  
BX200

DP-1295  
663324

AEC RESEARCH AND DEVELOPMENT REPORT

# ANALYSIS OF HYDROGEN EXPLOSION HAZARDS

J. B. PORTER



*Savannah River Laboratory*

*Aiken, South Carolina*

## NOTICE

This report was prepared as an account of work sponsored by the United States Government. Neither the United States nor the United States Atomic Energy Commission, nor any of their employees, nor any of their contractors, subcontractors, or their employees, makes any warranty, express or implied, or assumes any legal liability or responsibility for the accuracy, completeness or usefulness of any information, apparatus, product or process disclosed, or represents that its use would not infringe privately owned rights.

Printed in the United States of America  
Available from  
National Technical Information Service  
U. S. Department of Commerce  
5285 Port Royal Road  
Springfield, Virginia 22151  
Price: Printed Copy \$3.00; Microfiche \$0.95

ANALYSIS OF HYDROGEN EXPLOSION HAZARDS

by

J. B. Porter

Engineering Department  
Wilmington, Delaware

July 1972

E. I. DU PONT DE NEMOURS & COMPANY  
SAVANNAH RIVER LABORATORY  
AIKEN, S. C. 29801

CONTRACT AT(07-2)-1 WITH THE  
UNITED STATES ATOMIC ENERGY COMMISSION

### ABSTRACT

Tests were conducted with 30-50 vol %  $H_2$  in air at initial pressures from 1 to 12 atm abs on process pipes and tanks to determine the consequences of hydrogen-air deflagration and/or detonation in Savannah River process equipment. Deflagration-to-detonation transition can occur with 30-40 vol %  $H_2$  in air in pipes with cross-sectional area  $>0.304 \text{ in}^2$  at initial pressure  $\geq 1$  atm abs. The ratio of peak detonation pressure to initial pressure in  $\frac{1}{2}$ - and 2-inch pipes with 30-50 vol %  $H_2$  in air is  $\sim 25$  to 1. Peak pressure to initial pressure ratio in tanks for a deflagration is  $\sim 8$  to 1. The predetonation distance (the distance the flame travels from the point of ignition to the detonation point) is  $< 6$  ft at initial pressures  $\geq 1$  atm abs. Ignition energy of a detonation in  $\frac{1}{2}$ - and 2-inch pipe connected to a  $4\frac{1}{2}$ -ft-dia x 6-ft straight side tank with initial pressure  $\leq 10$  atm abs is not sufficient to cause a detonation in the tank. The ratio of peak pressure to initial pressure in the tank for a deflagration is  $\sim 8$  to 1.

## CONTENTS

	<u>Page</u>
Introduction . . . . .	7
Summary . . . . .	9
Discussion . . . . .	11
Deflagration-Detonation Processes . . . . .	11
Pipe Tests . . . . .	11
Tank Tests . . . . .	22
Preliminary Calculations . . . . .	22
Results . . . . .	24
Flame Arrester Tests . . . . .	34
Acknowledgments . . . . .	36
Appendix - Peak Pressure Calculations for Pipe Tests . .	37
References . . . . .	39

## LIST OF TABLES

<u>Table</u>		<u>Page</u>
I	Deflagration-Detonation Processes . . . . .	11
II	Results of Pipe Tests . . . . .	13
III	Strain Gage Readings and Calculated Pressure Peaks . . . . .	19
IV	Tank Analysis Calculations and Results . . . . .	22
V	Results of Tank Tests . . . . .	24

## LIST OF FIGURES

<u>Figure</u>	<u>Page</u>
1 Pipe Test Equipment Diagram . . . . .	14
2 Oscillograph Traces for Pipe Test 13 . . . . .	16
3 Strain Gage Locations and Oscillograph Traces for Pipe Test 3 . . . . .	18
4 Damaged 2-inch Pipe After 12-atm Test . . . . .	21
5 Ceramic-Metal Seal . . . . .	21
6 Tank Test Equipment Diagram . . . . .	25
7 Strain Gage and Photo Stress Locations . . . . .	26
8 Photo Stress Material . . . . .	28
9 Tank Before Test . . . . .	29
10 Tank After 3.1-atm Test . . . . .	29
11 Tank After 7-atm Test . . . . .	31
12 General Appearance of Tunnel After 10-atm Test . . . . .	33
13 Concrete Base of Tank After 10-atm Test . . . . .	33
14 Flame Arrester Test Equipment Diagram . . . . .	34





## INTRODUCTION

Tests were conducted to determine the consequences of hydrogen-air deflagration and/or detonation in Savannah River process equipment. Small concentrations of gaseous hydrogen are safe in the absence of air; however, any air leaks in the process equipment could cause an explosion-fire hazard.

The study, conducted by Carney's Point Development Laboratory, was based on the assumptions that in-leakage of air could occur in sufficient quantities to produce a stoichiometric hydrogen-air mixture (29.5 vol % H<sub>2</sub> in air) and that an ignition source could be available. A leak of this size would result from such sources as loose flanges or valve failures. Specific objectives considered in these tests were:

- Determine whether process pipes will withstand a detonation pressure peak of 116 times the initial pressure.
- Determine whether process tanks will withstand deflagration pressure peaks of 8 times the initial pressure.
- If tanks cannot withstand these pressures, specify modifications.
- Determine whether a hydrogen explosion originating in a pipe connected to a tank will cause an explosion in the tank.
- Investigate commercially available flame arresters for possible isolation of process steps to avoid propagation of deflagrations or detonations throughout the process.

No effort was made to perform a complete safety analysis or to investigate all possible implications of the data obtained.



## SUMMARY

Tests were conducted with 30 to 50 vol % hydrogen in air mixtures, at initial pressures from 1 to 12 atmospheres absolute in  $\frac{1}{2}$ - and 2-inch schedule 40, 304 stainless steel pipes and at initial pressures from 1.5 to 10 atm abs in a  $4\frac{1}{2}$ -ft-dia x 6-ft straight side 304 stainless steel tank. A summary of the results is given below:

- Deflagration to detonation transition can occur with 30 to 40 vol %  $H_2$  in air mixtures in pipes with cross-sectional area  $\geq 0.304$  in.<sup>2</sup> at initial pressure  $\geq 1$  atm abs.
- Peak detonation pressure to initial pressure ratio in  $\frac{1}{2}$ - and 2-inch pipes with 30 to 50 vol %  $H_2$  in air mixtures is approximately 25 to 1.
- Detonation pressures with initial pressures  $\leq 12$  atm abs are not sufficient to deform or rupture  $\frac{1}{2}$ -inch Schedule 40, 304 stainless steel pipe.
- Detonation pressures with initial pressure  $\leq 3$  atm abs are not sufficient to deform or rupture 2-inch Schedule 40, 304 stainless steel pipe.
- Detonation pressures with initial pressures of 12 atm abs are sufficient to deform but not rupture 2-inch Schedule 40, 304 stainless steel pipe.
- Normal 5 diameter pipe bends up to 90° have no apparent effect on the formation or propagation of detonation waves.
- The predetonation distance for 30 to 50 vol %  $H_2$  in air mixtures is less than 6-ft at initial pressures  $\geq 1$  atm abs.
- Detonation pressures in  $\frac{1}{2}$ -inch pipe with initial pressures  $\leq 12$  atm abs are not sufficient to damage a 2-inch vacuum flange and gasket or a  $\frac{1}{2}$ -inch globe valve.
- Detonation pressures in  $\frac{1}{2}$ -inch pipe with initial pressures  $\leq 1$  atm abs are not sufficient to damage a bourdon tube pressure gage (0-2300 mm Hg) or a glass-to-metal seal.

- Detonation pressures in  $\frac{1}{2}$ -inch pipe with initial pressure  $\geq 1$  but  $\leq 12$  atm abs are sufficient to deform but not rupture a bourdon tube pressure gage (0-2300 mm Hg) and a glass-to-metal seal.
- Ignition energy of a detonation in  $\frac{1}{2}$ - and 2-inch pipe connected to a  $4\frac{1}{2}$ -ft-dia x 6-ft straight side tank with initial pressure  $\leq 10$  atm abs is not sufficient to cause a detonation in the tank.
- The ratio of peak pressure to initial pressure in the tank for a deflagration is  $\sim 8$  to 1.
- Deflagration pressures with initial pressures equal to  $1\frac{1}{2}$  atm abs are sufficiently high to cause minor permanent deformation at the knuckle radius of the test tank.
- Deflagration pressure with initial pressure  $\geq 1\frac{1}{2}$  and  $\leq 7$  atm abs are sufficiently high to cause serious permanent deformation of the tank at the knuckle radius, heads, and walls, but no gas leaks.
- Tank deformation is of the type and in the pressure range predicted by stress analysis.
- Deflagration pressure with initial pressure  $\geq 10$  atm abs is sufficient to rupture the tank.
- A commercially available flame arrester mounted at points 16 inches and 2 ft from the point of ignition failed to stop deflagration propagation or detonation formation in  $\frac{1}{2}$ -inch pipes with initial pressures  $> 1$  atm abs.

## DISCUSSION

### DEFLAGRATION-DETONATION PROCESSES

Flame, as a physical phenomenon, is generally understood to be burning gas. Its prerequisite is the formation of a combustible mixture such as hydrogen and air. If such a mixture is ignited, a combustion wave propagates from the ignition to the adjacent layer of gas; in turn, each portion in the burning layer serves as an ignition source for the next adjacent layer, and so on. The mixture propagates a flame only above some minimum and below some maximum percentages of fuel gas. These percentages are called the lower and upper flammability limits. For a hydrogen-air mixture, these percentages are 4 and 73%, respectively.<sup>1</sup>

The combustion wave, or flame front, travels against the unburned mixture at a definite velocity. This velocity is a function of the mixture composition, increasing from zero at the two limits of flammability to a maximum at some intermediate percentage of fuel gas.<sup>2</sup> The flame front may propagate at a rate either subsonic (deflagration) or supersonic (detonation) relative to the unburned gas. Table I shows a comparison of deflagration and detonation processes.

TABLE I  
Deflagration-Detonation Processes

	<u>Deflagration</u>	<u>Detonation</u>
Flame Propagation Rate <sup>3</sup> (relative to unburned gas)	Subsonic	Supersonic
Rate of Pressure Equalization <sup>3</sup>	Sonic	< Flame Propagation Rate
$\Delta P$ Across Flame Front <sup>3</sup>	Relatively Small	Appreciable
Peak/Initial Pressure Ratio	Seldom Exceeds 8:1 <sup>4</sup>	Approximately 116:1

In the case of combustion in pipes, turbulent gas motion in the deflagration aids the heat transfer and accelerates progress of the deflagration front. The thermal expansion of the burning gas induces considerable flow with attendant pressure waves. With highly explosive mixtures, these pressure waves and the deflagration wave merge into a detonation wave, which constitutes a self-propelled shock wave travelling in the pipe at a velocity exceeding that of sound in the unburned gas.<sup>2</sup> The detonation velocity is a physical constant of the properties of the gas mixture and is little influenced by changes in the initial pressure, initial temperature, and pipe size (if the size is larger than a small limiting value).<sup>5</sup>

In deflagration, the pressure in the system will equalize at the speed of sound throughout the enclosure in which combustion is taking place, so the pressure drop across the flame front and the final peak pressure will be relatively small.<sup>4</sup> For detonations, the rate of pressure equalization will be less than the propagation rate and there will be an appreciable pressure drop across the flame front.<sup>3</sup> With the most combustible hydrogen-air mixtures, at ordinary temperatures, the ratio of peak pressure within the enclosure may be  $14\frac{1}{2}$  times higher for detonations than for deflagrations.

## PIPE TESTS

Pipe tests were conducted with 30 to 50 vol %  $H_2$  in air in  $\frac{1}{2}$ - and 2-inch Schedule 40, pipes of 304 stainless steel. The  $\frac{1}{2}$ - and 2-inch pipe sizes were chosen for testing because 90% of the piping in the process facility is of these sizes. The 30-50 vol % range was used because tests<sup>5</sup> indicated that it was the most explosively energetic. Six different piping configurations, two containing process components such as valves, and initial pressures from 1 to 12 atm absolute were used. Figure 1 shows test equipment diagrams, and Table II summarizes test results.

The test gas mixtures were prepared using a Greer accumulator and reservoir (Figure 1). In a typical test, the piping system was evacuated, and the required amounts of hydrogen and air were admitted to the isolated accumulator and reservoir. To mix the gases, the bladder of the accumulator was pressurized with nitrogen and vented at least five times to transfer the gas back and forth between the accumulator and the reservoir. After mixing, the gas was charged to the pipe system to the desired pressure.

TABLE II  
Results of Pipe Tests

Test	Test Configuration	Vol % H <sub>2</sub> <sup>a</sup>	Initial Pressure, psia	Peak Pressure, psia <sup>b</sup>	P <sub>p</sub> /P <sub>i</sub>	Maximum Flame Velocity, ft/sec <sup>a</sup>	Detonation Range	Damage to Equipment
1	1/2-inch Sch. 40 pipe, 40 ft straight (Figure 1a)	30	29.7	580	19.53	5870	Yes	No
2		30	55.7	1155	20.74	6060	Yes	No
3		30	74.7	1460	19.54	5890	Yes	No
4		30	73.5	1500	20.41	d	Yes	
5		30	73.5	1500	20.41	d	Yes	
6		30	73.5	1500	20.41	d	Yes	1500-psi rupture disc
7		30	73.5	1500	20.41	d	Yes	failed
8		30	37.7	1500	39.79	d	Yes	1500-psi disc did not fail
9		30	56.2	1500	26.69	d	Yes	1500-psi disc
10		40	74.7	1500	20.08	d	Yes	failed
11	1/2-inch Sch. 40 pipe, 40 ft straight with 2 90° bends (Figure 1b)	40	37.7	750	19.89	d	Yes	750-psi disc
12		40	37.7	885	23.47	6446	Yes	failed
13		40	74.7	1745	23.36	6421	Yes	1500-psi disc failed
14		39.5	44.7	1105	24.72	6610	Yes	No
15		39.5	44.7	1120	25.06	6647	Yes	No
16		39.5	44.7	1100	24.61	6603	Yes	No
17		39.0	44.7	1025	22.93	6365	Yes	No <sup>e</sup>
18		39.0	44.7	1095	24.50	6588	Yes	No <sup>e</sup>
19		39.0	44.7	1040	23.27	6425	Yes	No <sup>e</sup>
20		39.5	14.7	265	18.03	5643	Yes	No <sup>f</sup>
21	2-inch Sch. 40 pipe, 40 ft straight (Figure 1c)	39.5	29.4	955	32.48	7575	Yes	No <sup>f</sup>
22		39.5	44.7	1295	28.97	7150	Yes	No <sup>f</sup>
23		39.0	176.4	4140	23.47	6445	Yes	No <sup>f</sup>
24		36.6	14.7	180	12.24	4680	Yes	No <sup>g</sup>
25	Flame arrester (Figure 22)	36.6	44.7	825	18.46	5715	Yes	No <sup>g</sup>
26	'Y' Piece (Figure 1d)	38.0	44.7	1330	29.75	7250	Yes	No <sup>h</sup>
27	Component tests in 1/2-inch pipe (Figure 1e)	38.5	14.7	310	21.09	6110	Yes	No <sup>i</sup>
28		38.5	29.4	615	20.92	6080	Yes	Gage ruined <sup>i</sup>
29		39.0	43.1	890	20.65	6050	Yes	Gage distorted <sup>i</sup>
30		39.0	86.2	1650	19.14	5820	Yes	Gage distorted <sup>i</sup>
31		39.0	172.4	3455	20.04	5960	Yes	Gage distorted <sup>i</sup>
32		37.8	14.7	225	15.31	5190	Yes	No <sup>i</sup>
33		37.8	29.4	550	18.71	5755	Yes	Seal distorted <sup>i</sup>
34		39.2	43.1	490	11.37	4485	Yes	Seal distorted <sup>i</sup>
35		39.2	172.4	4595	26.65	6865	Yes	Seal distorted <sup>i</sup>

a. Estimated for Tests 1-13. Measured by mass spectroscopy for Tests 14-35.

b. Calculated from flame speeds. See Appendix.

c. Average for detonation range. Based on ionization probe data.

d. Equipment check tests with rupture discs. No probes connected.

e. Flame appeared to slow slightly when passing through bends.

f. Micrometer readings at machined flats on end of pipe revealed no change after tests.

g. Arrester did not stop flame.

h. Configuration did not affect flame.

i. Flame arrester not effective. No damage to valve or flange. None of the components leaked.





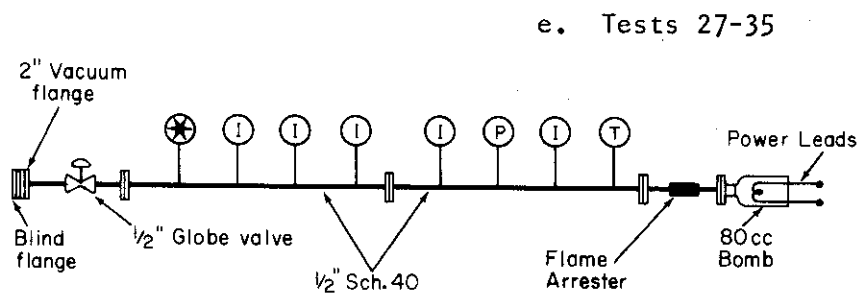
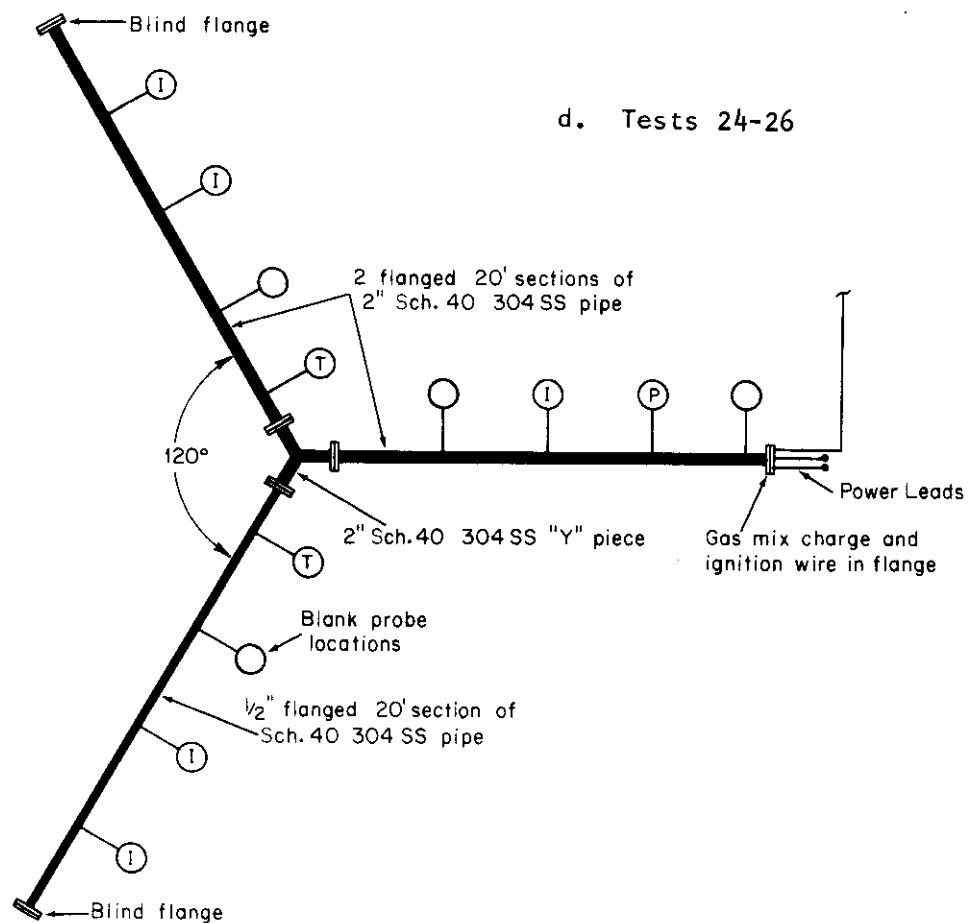


FIGURE 1 (CONTINUED)

The reaction velocity was determined by measuring the time required for the reaction to travel a measured distance between ionization probes. A probe consists of two insulated electrodes, with a gap of 1/16 inch, at a potential of 1200 v. Passage of a shock or flame front causes ionization in the gas between the electrodes, which in turn permits the electrodes to discharge. The time of that event is recorded on a Midwestern Model 801 oscillograph. Figure 2 shows an example of probe data for a typical test. These traces show probe response to flame (reaction) front passage, and by setting the oscillograph chart speed to a known value (128 in/sec), the average velocity between probes was calculated. As shown in Table II, all calculated speeds were in excess of 4000 ft/sec. This is clearly in the supersonic range (the speed of sound in the unburned mixture is approximately 1450 ft/sec) and indicates detonation occurred in all tests.

The ionization probe traces indicated that the reaction propagation rate increased to detonation level before reaching Probe 2, located 6 ft from the ignition source. The test equipment was not set up to synchronize trace recordings and time of ignition, and as a result, it was impossible to accurately determine the distance required for the flame to increase in speed from ignition to detonation velocities. However, the distance is <6 ft (predetonation distance  $\leq 6$  ft).

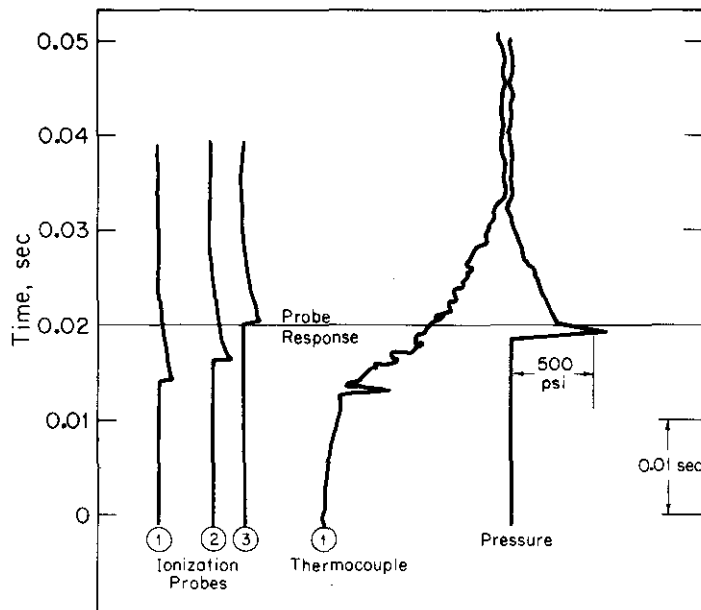


FIGURE 2. Oscillograph Traces for Pipe Test 13

A Kistler Model 601H pressure transducer was used in an attempt to determine peak pressures and rate of pressure rise. The transducer's response was not fast enough to indicate the rate of pressure rise or peak pressure, and as a result, the peak pressures were calculated from a relationship of pressure peak to flame speed. Using flame speed values obtained by the procedures discussed above, the peak pressures were calculated as shown in the Appendix.

The average calculated ratios of peak pressure to initial pressure were  $\sim 25$  to 1 rather than the predicted value of 116 times initial pressure. Because the calculated values disagreed with predicted values, two additional series of tests were made to verify the calculated maximum pressure values.

The first series was conducted with accurately rated rupture discs (rupture pressure  $\pm 5\%$  of rated value) installed at the end of the  $\frac{1}{2}$ -inch pipe system (Figure 1a). With the initial pressure set at 74.7 psia, a 1500-psia rupture disc failed, indicating the final to initial pressure ratio was  $>20$  to 1. The calculated value for this test was 23.36. The initial pressure was then reduced to 37.7, and a 1500-psia disc did not fail, indicating that the ratio was not as great as 38 to 1. The calculated value for this test was 23.47 to 1. Finally, the 1500-psia disc was replaced with one rated at 750 psi, and the test at 37.7 psia was rerun. The 750-psi disc failed, indicating the ratio was in excess of 19 to 1 and, as shown above, the calculated value was 23.47 to 1. While this series of tests did not validate the calculated results exactly, it did show that they were in the right range and were much lower than the predicted 116 to 1.

The second series was conducted to obtain values that could be compared directly to the calculated values. A variable wall thickness section was fabricated from a 3 ft length of 2-in.-dia heavy-wall 304 stainless steel tubing. The inside diameter of the tube was not changed, but the outside diameter was machined over 12-inch portions to give wall thicknesses equal to, 30% greater than, and 30% less than the wall thickness of Schedule 40 pipe. The three sections were instrumented with strain gages, and the pipe was installed in the middle of the 2-inch pipe system. The pipe section design and strain gage locations are shown in Figure 3. When the pipe was subjected to detonation tests, the strain gage measurements were recorded and used to calculate the system pressure.

An example of the probe and gage traces is shown in Figure 3. The strain gage readings and calculated pressures are shown in Table III. The values are in the correct range. This correlation and the results of the first test series indicate that the calculated values are accurate within experimental error.

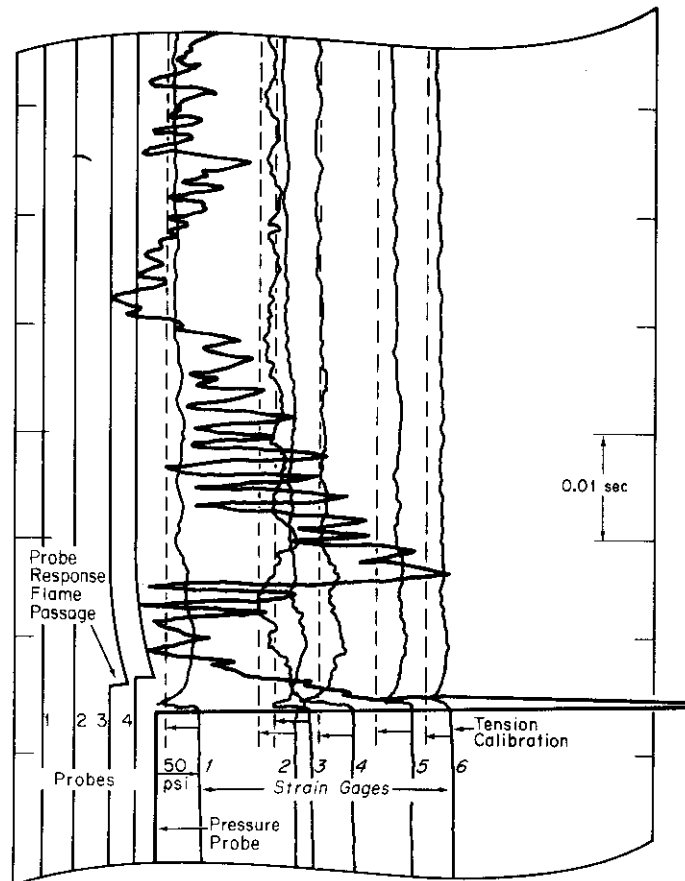
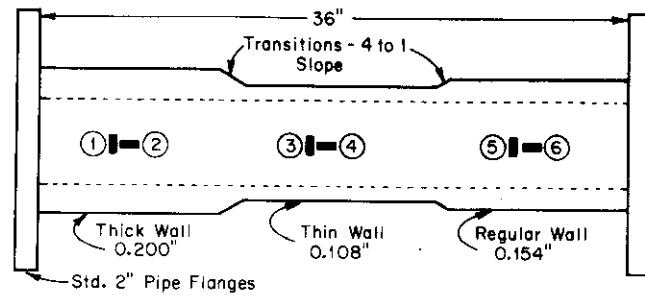


FIGURE 3. Strain Gage Locations and Oscillograph Traces for Pipe Test 3

TABLE III

## Strain Gage Readings and Calculated Pressure Peaks

Wall Thickness (t)	0.200	0.108	0.154				
Mean Radius (R)	1.100	1.054	1.077				
(t/R)	0.182	0.1025	0.144				

	Strain Gage Readings						Pressure Probe Readings
	1	2	3	4	5	6	
$1\frac{1}{2}$ atm <sup>a</sup>							
Strain, $\mu$ in/in	75	0	132	140	105	117	
Stress, psi	2250	675	5250	5400	4100	4560	
Calc Pressure, psi	410		540		586		225
3.0 atm <sup>a</sup>							
Strain, $\mu$ in/in	150	33	165	245	140	112	
Stress, psi	4830	2500	7430	9000	5230	4620	
Calc Pressure, psi	873		763		750		630
6.0 atm <sup>a</sup>							
Strain, $\mu$ in/in	315	0	278	406	210	242	
Stress, psi	9460	2840	12000	14700	8500	9160	
Calc Pressure, psi	1720		1230		1210		840

a. Pressure peaks calculated by methods in Appendix

$1\frac{1}{2}$  atm abs test — 440 psia

3 atm abs test — 695 psia

6 atm abs test — 1299 psia

All  $\frac{1}{2}$ -inch test piping withstood test pressures with initial pressures to 12 atm abs without measurable deformation. Introduction of pipe bends up to 90° and a combination of  $\frac{1}{2}$ - and 2-inch pipe in a Y configuration had no apparent effect on the formation or propagation of detonation waves.

All 2-inch test piping withstood test pressures with initial pressures to 12 atm abs without measurable deformation when tested in the standard test configuration (2 connected, straight, 20 ft lengths). Introduction of the variable wall thickness section in the system and problems with preignition of the gas mixture in the pipe resulted in two bulges in the pipe in two of eight tests at initial pressure of 12 atm abs. One bulge occurred 20 ft from the ignition end of the pipe, adjacent to the multi-wall thickness section. The gasket at the connection was destroyed. The original outside diameter and the bulge o.d. were 2-3/8 and 2-9/16 inches, respectively. The second bulge (Figure 4) occurred several tests later at the extreme end of the pipe opposite the ignition end. The gasket on the blank flange was destroyed. The pipe bulged to 3-3/16 inch o.d.

After the pipe tests demonstrated the ability of the pipes to contain detonation pressures with initial pressure considerably greater than the maximum plant operating pressure, selected auxiliary components were tested to determine whether any of these components were a weak point in the system. The components tested included an Ashcroft bourdon gage, Model 1079SV, with a 0- to 2300-mm Hg range; a Powell  $\frac{1}{2}$ -inch inside screw Belloseal globe valve; a Latronics Corporation Style 99-2203 ceramic-metal seal; and a 2 inch vacuum flange and gasket. All components were mounted near the end of the  $\frac{1}{2}$ -inch pipe system (Figure 1e). The ceramic-metal seal was provided with a special holder (Figure 5) so that it could be installed in the piping system.

All components were tested with initial pressures from 1 to 12 atm abs. The valve and 2-inch flange assembly showed no evidence of damage from the detonations. The gage was serviceable following the test at 1 atm. Although the tube became progressively more distorted as the initial pressures were increased, it never ruptured. The seal did not leak in any tests, but it was badly deformed and near the point of structural failure following the 12-atm test.

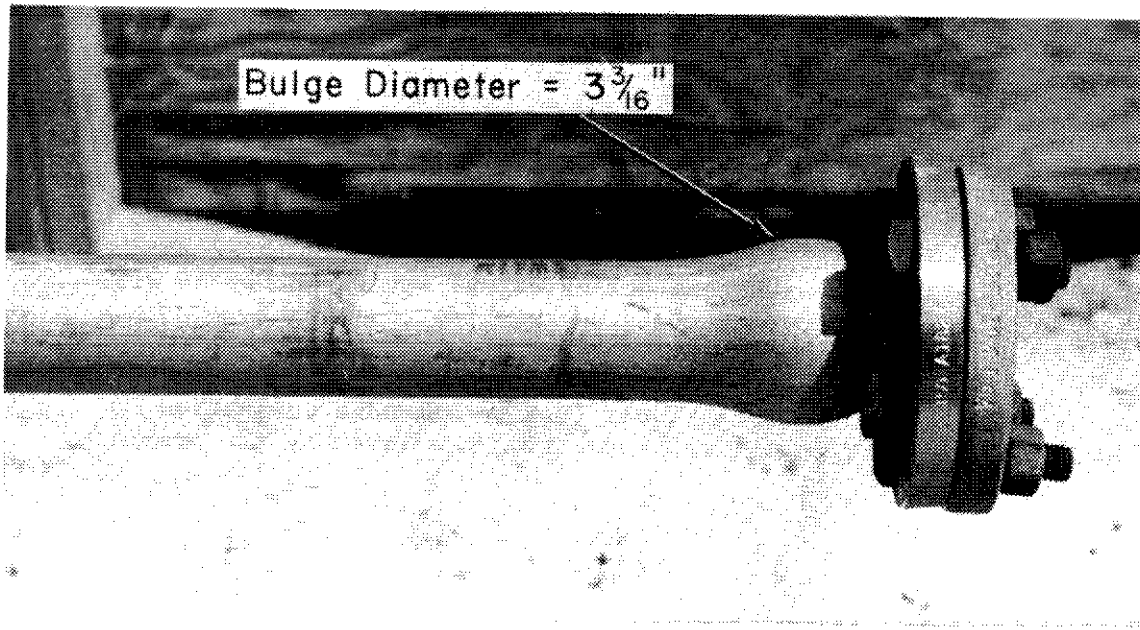


FIGURE 4. Damaged 2-inch Pipe After 12-atm Test

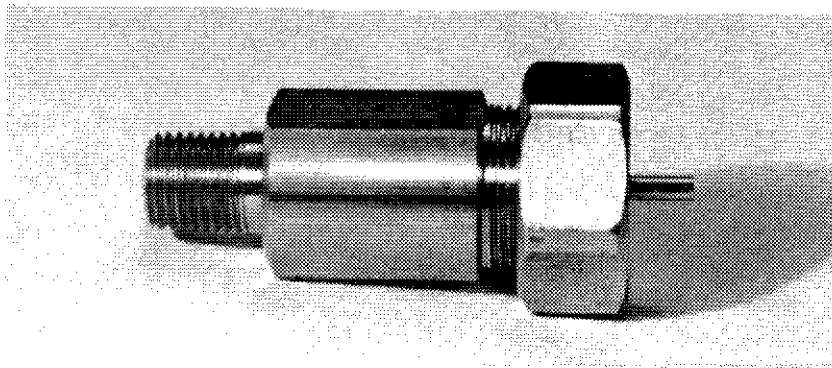
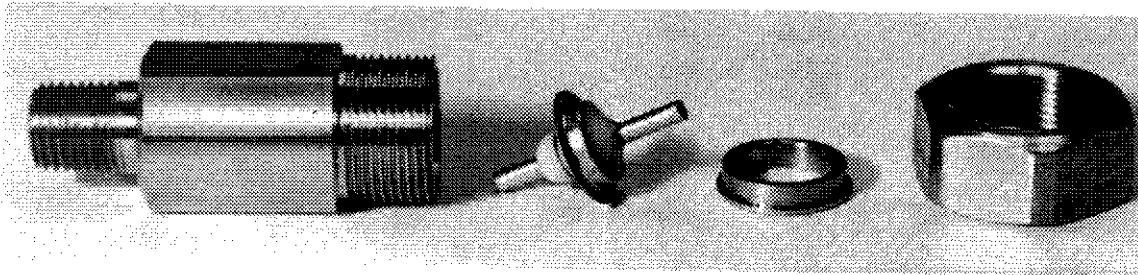


FIGURE 5. Ceramic-Metal Seal

## TANK TESTS

### Preliminary Calculations

Calculations to determine the ability of process tanks to withstand H<sub>2</sub>-air deflagration were made assuming a maximum pressure of 8 times the design pressure. The results of these calculations are shown in Table IV. Four of the 20 tanks reviewed are able to withstand deflagration, but the other 16 will undergo plastic deformation at the knuckle.

The equivalent pounds of TNT required to produce the shell pressures is also shown in Table IV. Recommended separation distances for TNT equivalent quantities are given by the American

TABLE IV  
Tank Analysis Calculations and Results

Construction Material	Design Temperature, °F	Strength at Design Temperature, psi		Design Pressure, psia	Tank Volume, ft <sup>3</sup>	Static Behavior of Shell, psia		Explosion Pressure, psia <sup>a</sup>
		Yield	Ultimate			Yield	Ultimate	
202 304	200	52,000 25,600	104,000 75,000	49.7	84	570 288	850 469	397.6
202 304	200	52,000 25,600	104,000 75,000	51.7	54	825 413	1230 677	413.6
304	200	25,600	75,000	49.7	55	220	355	397.6
202 304	200	52,000 25,600	104,000 75,000	59.7	19.2	952 476	1465 780	477.6
304L 304L	75	25,000	70,000	14.7	0.44	1005	1665	117.6
202 304	200	52,000 25,600	104,000 75,000	59.7	37.6	763 383	1175 625	477.6
304	75	30,000	75,000	14.7	2.25	1255	2000	117.6
202 304	200	52,000 25,600	104,000 75,000	59.7	11.85	952 476	1465 780	477.6
304	200	25,600	75,000	49.7	36.3	323	520	397.6
304	75	30,000	75,000	80.0	18.4	718	1015	640.0
202 304	200	52,000 25,600	104,000 75,000	59.7	11.85	952 476	1465 780	477.6
SA285C	650	21,800	55,000	124.7	58.6	407	645	997.6
202 304	200	52,000 25,600	104,000 75,000	49.7	81.2	570 288	850 469	397.6
SA285C	Ambient	27,000	55,000	14.7	105,000	49.2	65.7	117.6
SA285C	Ambient	38,000	70,000	14.7	132,630	52.7	71.7	117.6

a. This value is 8 times the design pressure.



Table of Distance for storage of explosives both for inhabited and uninhabited buildings, barricaded and nonbarricaded (Table IV). A comparison of these values with existing building space limitations indicated that barricading is impractical.

The tank chosen for the test is the weakest (second tank listed in Table IV). The calculations indicated failure due to plastic collapse at the knuckle would occur at only 42.7 psia. It was assumed that if this tank could hold the pressure peaks, all other tanks examined, and shown to be stronger, would also hold. The actual tests in the tunnel showed the tank began to deform at the knuckle during Test 1 (Table V), at the pressure level and by the deformation mechanism predicted by the calculations.

TABLE IV (Continued)

Construction Material	Static Strength of Heads						American Table of Distance for Maximum TNT Quantities			
	Plastic Collapse Knuckle, psia	Spher. Caps		TNT Equivalent,		Maximum Pressure For Collapse, psia	Inhabited, ft		Uninhabited, ft	
		Yield, psia	Burst, psia	Static Burst	At Expl. Pressure		Barricaded	Non Barricaded	Barricaded	Non Barricaded
202	70.7	-	-	24.20	9.50	314.7	125	250	11	22
304	42.7	-	-	11.95			110	220	10	20
202	198.7	-	-	39.00	6.36	171.5	140	280	12	24
304	105.7	-	-	11.58			110	220	10	20
304	-	-	-	5.83	6.22	131.7	90	180	8	16
202	254.7	-	-	11.2	2.70	226.7	110	220	10	20
304	132.7	-	-	4.98	2.70		70	140	6	12
304L	829.7	1727	2835	0.28	0.01	331.5	<70	70	<6	6
202	209.7	-	-	15.9	5.3	131.2	110	220	10	20
304	110.7	-	-	7.2	5.3		90	180	8	16
304	614.7	690	1095	1.78	0.05	806.7	70	140	6	12
202	254.7	-	-	6.46	1.67	319.7	90	180	8	16
304	132.7	-	-	3.12			70	140	6	12
304	105.3	-	-	5.66	4.08	133.7	70	140	6	12
304	263.7	-	-	11.95	9.50	174.7	110	220	10	20
202	254.7	-	-	6.42	1.66	19.70	90	180	8	16
304	132.7	-	-	3.12			70	140	6	12
SA285C	207.0	-	-	11.70	20.0	584.7	110	220	10	20
202	70.7	-	-	23.0	9.10	180.7	125	250	11	22
304	42.7	-	-	10.95			110	220	10	20
SA285C	-	352.7	555.7	978	2360	16.2 at 4 ft	Tank is Underground			
SA285C	-	488.7	-	-	-	-	-	-	-	-

## Results

The tank tests were conducted in two phases. In Phase 1, 40 vol % H<sub>2</sub> in air gas was used at 1- $\frac{1}{2}$ , 2- $\frac{1}{2}$ , and 3 atm abs. A detonation in a  $\frac{1}{2}$ -inch Schedule 40 pipe was allowed to propagate into a tank (Tests 1-3). In the second phase, the same H<sub>2</sub>-air mixtures were used at 1- $\frac{1}{2}$ , 2- $\frac{1}{2}$ , 3, 4- $\frac{1}{2}$ , 7, and 10 atm abs. A detonation traveling in a 2-inch Schedule 40 pipe was allowed to propagate into the same tank (Tests 4-9). Figure 6 shows a schematic diagram of the test equipment. Table V shows individual test data and results.

The gas mixtures were charged to the tank using an over-pressure technique. The desired 40/60 composition was formed using partial pressures and charging the tank to an initial pressure greater than the required test pressure. After allowing time for random mixing in the tank, the excess H<sub>2</sub>-air mixture was vented through the feed line in order to fill the ignition pipe and bomb with flammable mixture.

TABLE V  
Results of Tank Tests

Test	Pipe Diameter, inches <sup>a</sup>	vol % H <sub>2</sub> <sup>b</sup>	Initial Pressure, psia	Peak <sup>c</sup> Pressure, psia	Tank, P <sub>p</sub> /P <sub>i</sub>	Tank $\Delta P/\Delta t$ , (psi/sec)	Propagation Velocity, ft/sec		Detonation Range		Damage to Tank	Residual System Pressure, psig	Final <sup>f</sup> System Temperature, °F	Damage
							Pipe <sup>d</sup>	Tank <sup>e</sup>	Pipe	Tank				
1	$\frac{1}{2}$	35.8	22.0	165.5	7.51	4,510	6,727	106	Yes	No	Minor	2	120	No visible
2	$\frac{1}{2}$	39.1	33.1	263.1	7.96	9,560	6,617	145	Yes	No	Minor	14	g	No visible
3	$\frac{1}{2}$	40.4	45.7	384.7	8.40	16,500	6,800	591	Yes	No	Major	30	g	Visible
4	2	29.6	22.0	338.0	15.30	14,200	h	e	Yes	No	Major	g	g	No additional
5	2	33.0	33.1	191.0	5.80	6,500	7,610	e	Yes	No	Major	g	g	No additional
6	2	23.5	44.1	i	i	i	i	i	Yes	No	Major	g	g -	Progressive deformation
7	2	10.4	66.1	483.0	7.30	13,380	7,185	e	Yes	No	Major	g	g	at the knuckle
8	2	23.4	103.0	1085.0	10.50	-	7,745	e	Yes	No	Major	g	g -	radius sides and heads - No leaks
9	2	48.3	147.0	-	-	-	-	-	Yes	No	Destroyed	-	-	Ruptured into 4 major pieces

a. See Figure 6 for detailed layout of Tests 1 through 9.

b. Determined by mass spectroscopy. Suspect sample handling error in Tests 6, 7, and 8.

c. Measured by pressure transducer.

d. Average for detonation range.

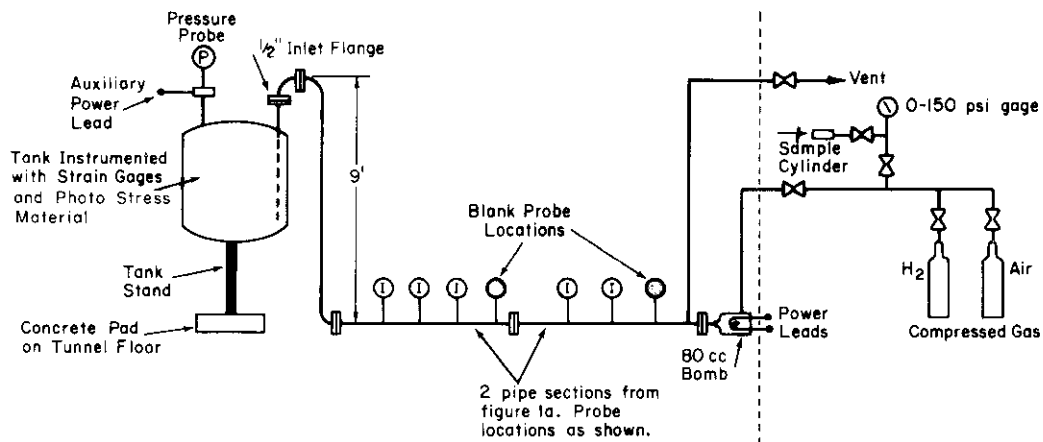
e. Calculated from tank geometry and pressure probe response. Probe did not recover fast enough in 2-inch pipe tests to permit similar treatment.

f. Estimated from tank wall temperature.

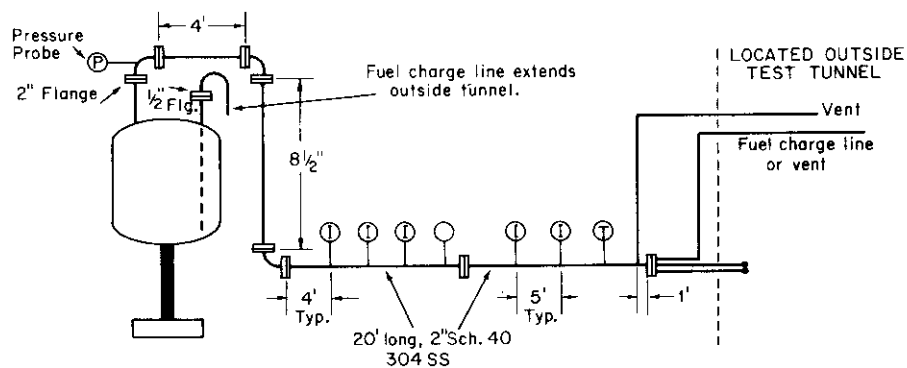
g. Not measured.

h. Probe malfunction.

i. Unexplained ignition delay. Suspected misfire. The oscillograph stopped just before audible explosion.



a. Tests 1-3



b. Tests 4-9

FIGURE 6. Tank Test Equipment Diagram

Following the first test, the tank contained residual hydrogen (because of fuel rich compositions) and nitrogen. Each subsequent test mixture was prepared by first adding  $O_2$  (to form the required  $N_2/O_2$  ratio) and then the additional air and hydrogen. In later tests at high pressures, all residual gases were removed by vacuum pump, and each new mixture was prepared as described for the first test.

The pressure peaks in the tank were measured with a pressure transducer and recorded on an oscillograph. These measured peak pressures give peak to initial pressure ratios in the tank of approximately 8 to 1. This is the value predicted for deflagration.<sup>5</sup>

Because preliminary calculations indicated that the test tank should deform, the tank was instrumented with strain gages and photo stress material to study the tank deformation as completely as possible.<sup>1</sup> Figure 7 shows gage and photo stress material locations and recorded maximum strain values at each gage location during Tests 1 through 3. Figure 7 also shows gage locations for Tests 4 through 9. The gages used are of a standard type and are designed to cover the range of elongation below 1%. Two types of photo stress material were used: Type I functioned at the 1% elongation level, and Type II covered the range from 1% to 3% elongation.

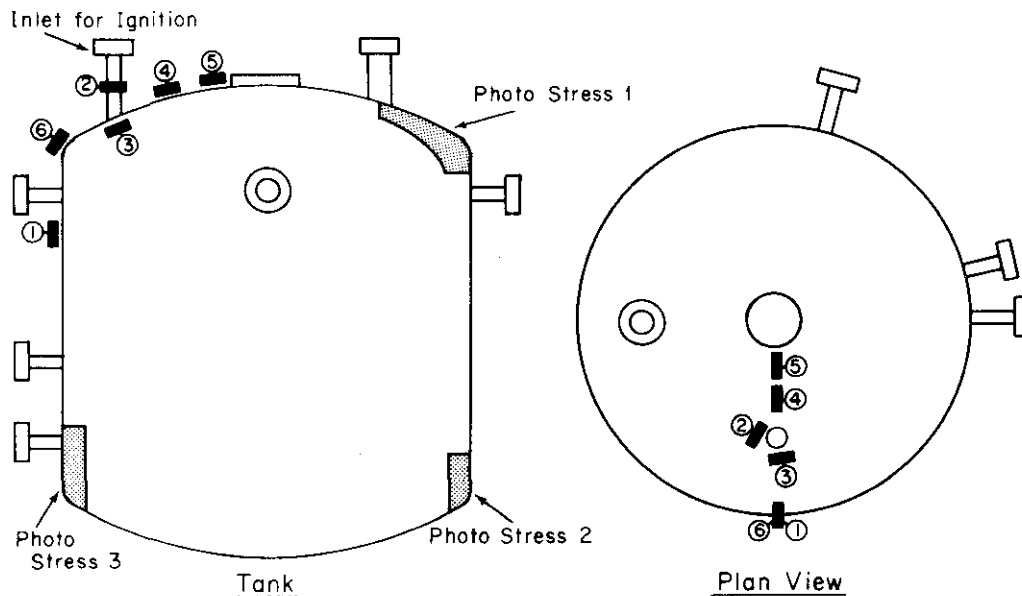


FIGURE 7. Strain Gage and Photo Stress Locations

At initial test pressures of  $1\frac{1}{2}$  and  $2\frac{1}{4}$  atm (Tests 1 and 2), the gages and photo stress indicated minor (nonvisible) permanent deformation at the knuckle. Peak strain values at the knuckle (Gage 6 on Figure 7) were above  $1100 \mu\text{in/in}$  for Tests 1 and 2, indicating the yield strength of the 304 stainless steel tank had been exceeded. In addition, the gage showed a zero shift, indicating permanent deformation in the tank at the knuckle. Gages on the body and head cap of the tank showed no zero shift.

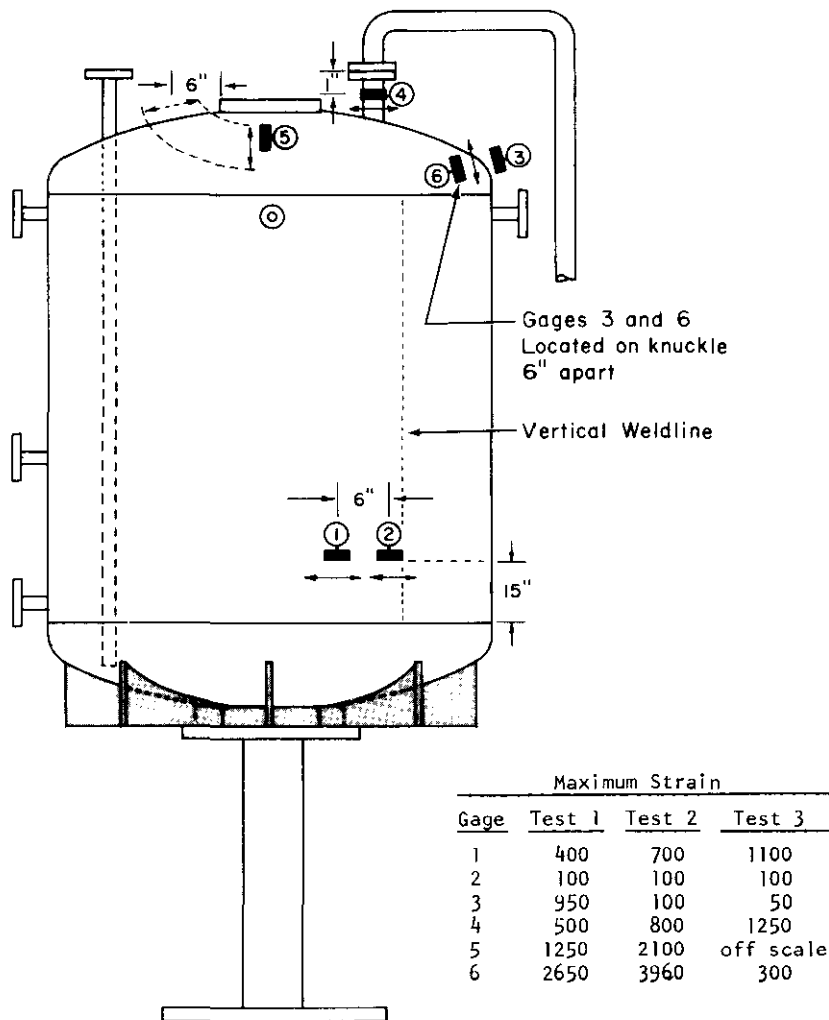


FIGURE 7 (CONTINUED)

The strain gage data were confirmed by the photo stress material. Figure 8 shows the photo stress material at the upper and lower knuckles after Tests 1 and 2. Both types of material cracked, or in the case of Test 2, popped off the tank completely. Brightly colored areas on the material indicate stress buildup due to wall and head material deflection. The maximum stress is at the knuckle radius, as predicted by stress calculations and indicated by strain gages.

At initial test pressure of 3 atm abs (Test 3), serious (visible) permanent deformation of the knuckle, head cap, and walls occurred. Data from the strain gages and photo stress material was of limited value due to the rapid heat buildup and deformation causing all gages and photo stress material to pop off the vessel. However, initial trace values did indicate that the yield strength of the material (1100 psi/in) was exceeded at the knuckle (Gage 6), head cap (Gage 4), and sidewalls (Gage 1). Visual deformation was also apparent at all areas mentioned above. Figure 9 shows the tank before testing; Figure 10 shows the tank after Test 3.

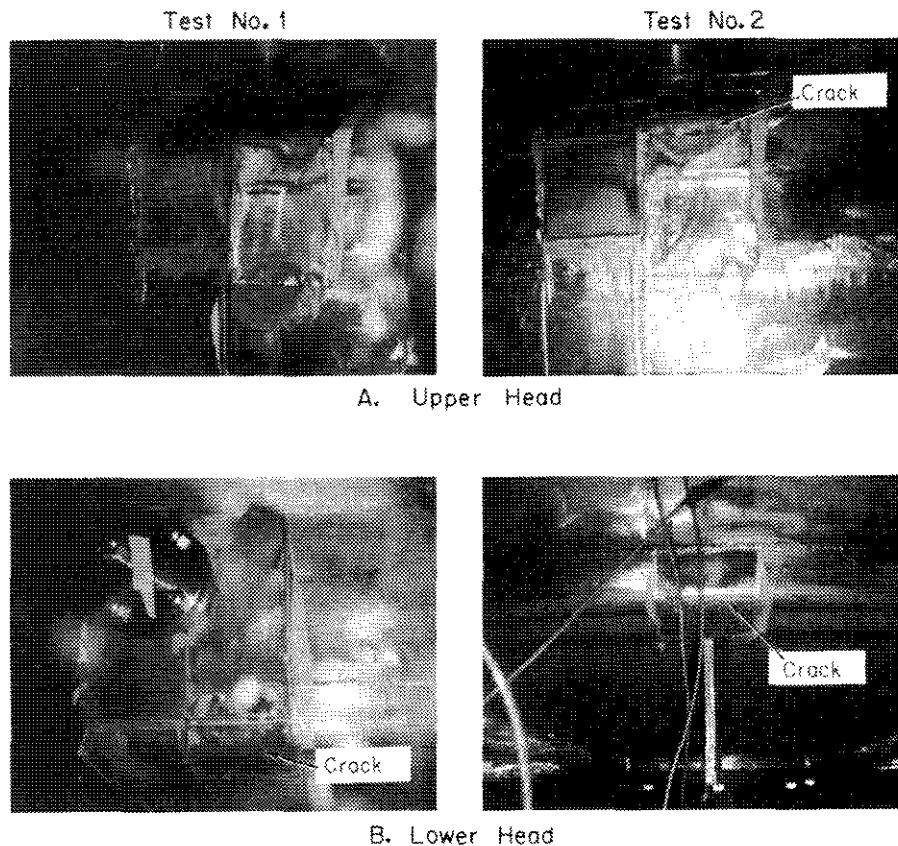


FIGURE 8. Photo Stress Material

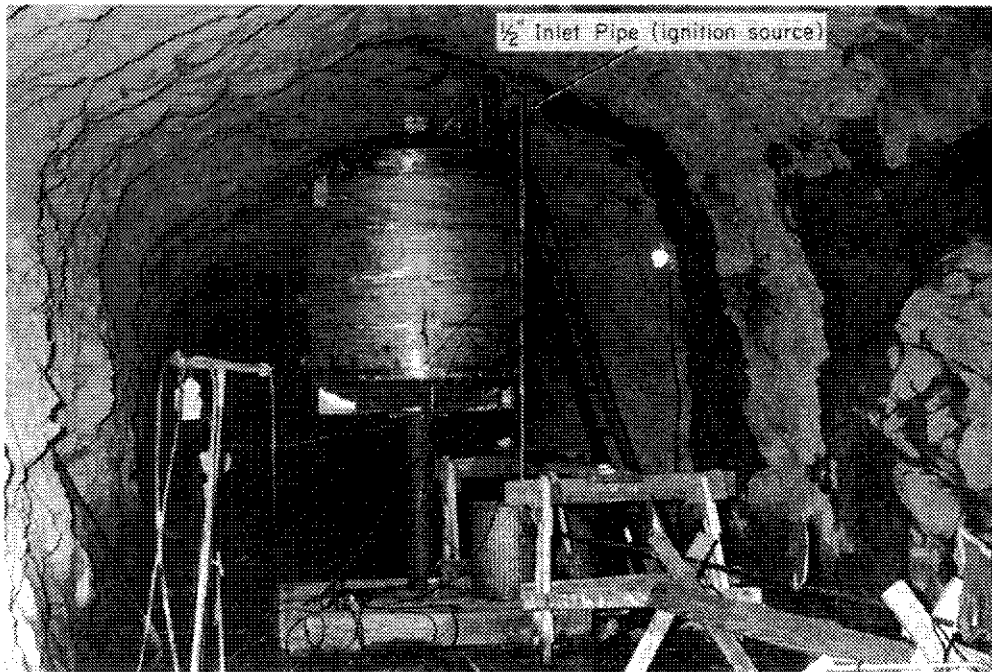


FIGURE 9. Tank Before Test

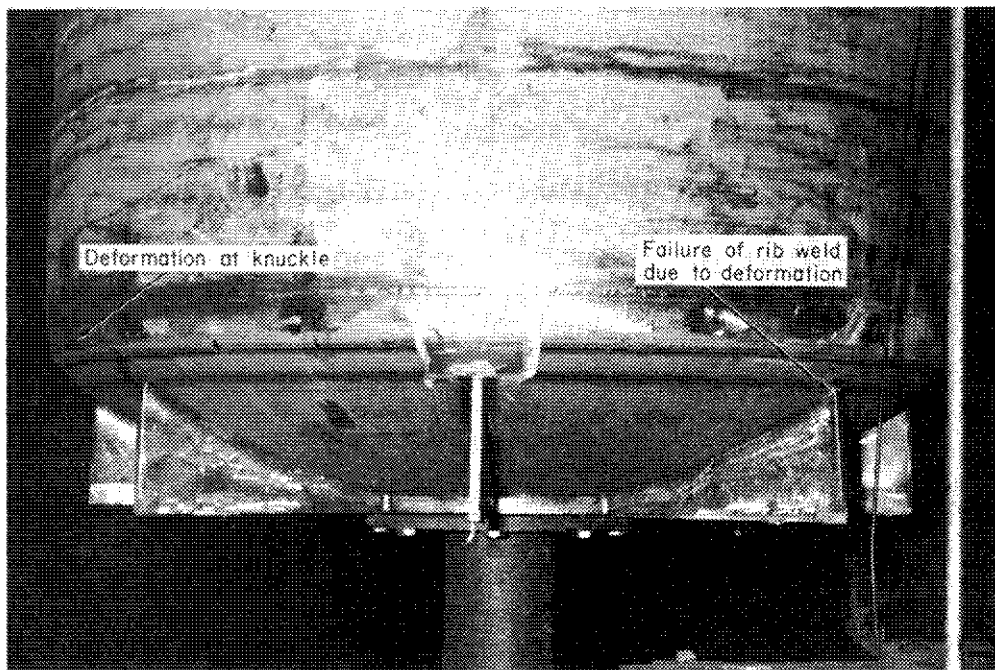


FIGURE 10. Tank After 3.1-atm Test

In Tests 4 through 9, the shock front was introduced to the tank from a 2-inch pipe. The pressure transducer was mounted on the 2-inch pipe just above the tank (see Figure 6). The transducer did not have sufficient time to recover from passage of the shock front from the pipe to give highly reliable pressure data. This fact explains the spread in the  $P_p/P_i$  ratios (Table IV) and is also the reason an estimate could not be made of the propagation velocities inside the tank.

No additional visible damage occurred during Tests 4 and 5, conducted at  $1\frac{1}{2}$  and  $2\frac{1}{4}$  atm abs, respectively. However, while the strain gages showed no additional yielding during Test 4, general yielding was observed during Test 5.

A number of misfires were experienced in Test 6, which was conducted at 3 atm abs. Ignition was delayed until after the oscillograph was stopped. As a result, no data were obtained. The test was not repeated.

During tests at  $4\frac{1}{2}$  and 7 atm (Tests 7 and 8) deformation at the heads, sidewall, and knuckles progressively increased. After Test 7, the tank circumference increased from 171 to 175 inches, and after Test 8, the circumference increased to 208 inches. The strain gage traces indicated the deformation was fairly uniform. After the 7-atm test (Figure 11) the originally straight sides of the tank were rounded, the knuckle radius was increased, and the top and bottom heads bulged. Fairly uniform ripples in the circumference at the knuckle, with some of the ripples coinciding with the rib welds and a rib weld failure, are visible in Figure 11. A similar ripple near the base of the 2-inch nozzle on the top of the tank can be seen in Figure 11.

Although serious deformation occurred during Tests 1 through 8, the tank did not rupture or leak. At the end of each test a residual pressure was caused by temperature effects on unburned tank gases; absence of pressure loss indicated the integrity of the vessel had not been destroyed.

The strain gage traces for Tests 7 and 8 showed that several of the gages behaved abnormally. In Test 7, Gage 1 gave a large compressive strain. The circuit for Gage 1 probably failed, and it was replaced. In Test 8, Gages 1, 2, and 5 increased to a peak and then abruptly dropped to normal. Subsequent inspection showed that the adhesive for those gages had failed. The circumference of the tank just above Gages 1 and 2 had increased to 208 inches. This increase corresponds to a new tank diameter of  $5\frac{1}{2}$  ft. The tank diameter had increased by 1 ft during Tests 7 and 8, and the strain was 12% during Test 8.



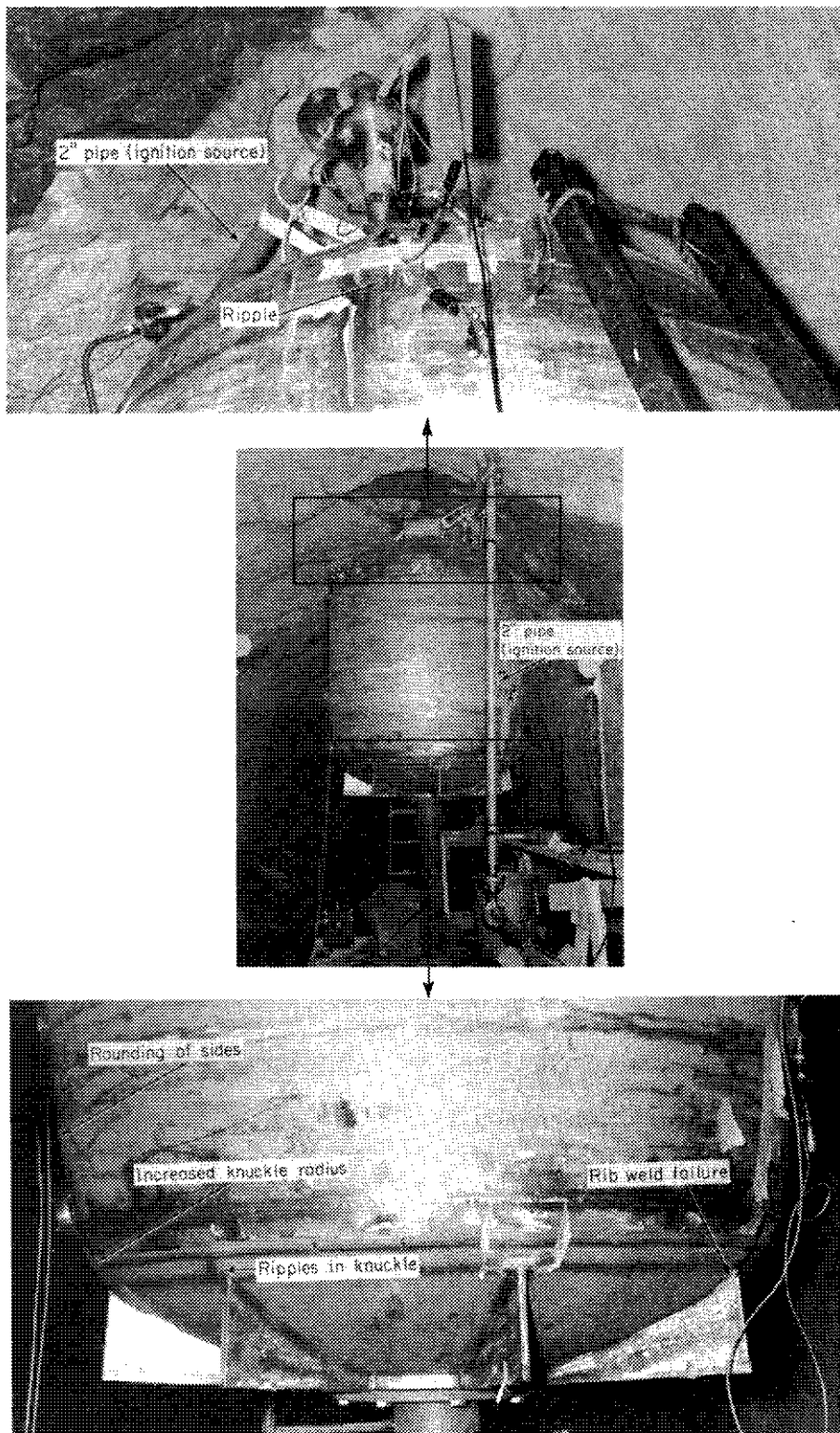


FIGURE 11. Tank After 7-atm Test

In Test 9, the tank was destroyed at 10 atm abs initial pressure. It failed by rupturing into four approximately equal sized sections. One section came to rest about 5 ft inside the tunnel entrance (the tank had originally been located 125 ft inside the tunnel). A second piece was found 35 ft toward the entrance and the third and fourth pieces were blown 50 and 65 ft to the rear of the original tank location. The general appearance of the tunnel following the explosion is shown in Figure 12, and the concrete base on which the tank was mounted is shown in Figure 13. The condition of the tank remains indicates that the reaction in the tank was a deflagration and not a detonation.

Oscillograph traces for Test 9 show that the tank ruptured within 0.02 sec after strain gage signals showed an increase in tensile strain. These traces also show that the probes located in the pipe responded after the tank had ruptured and in reverse order, apparently indicating that the ignition originated in the tank and not in the pipe. However, the tank probably did not undergo a spontaneous ignition. The probes must have failed to respond to the flame front passage in the pipe and were triggered by debris from the ruptured tank striking the exterior ends of the probes.

A fragment was removed from the ruptured tank and was subjected to a metallurgical examination. Hardness readings on various areas on the fragment varied from Rockwell C-23 to 30. For comparison, the hardness of annealed Type 304 stainless steel is Rockwell B-75 to 90, which is much lower in hardness than the test fragment. These hardness readings indicate that the stainless steel had been severely cold-worked during the repeated explosion testing, resulting in a rise of tensile and yield strengths and in a decrease in the ductility. No tensile tests were made; however, based on the observed hardness, it is estimated that the tensile strength in the most severely deformed areas was raised from 75,000 psi to 110,000-120,000 psi.

A microscopic examination of the stainless steel structure disclosed that the amount the metal was cold-worked varied from area to area, although all areas gave evidence of some cold-work. Grains were found to be distorted and some showed strain lines.

As the tank was tested, the stainless steel was work hardened, which resulted in an increased mechanical strength and reduced ductility. Although the ductility was reduced, it had not been reduced to the point that the stainless steel would be considered brittle.

The tank used in the tests apparently contained no serious defects because it withstood pressures many times its design



FIGURE 12. General Appearance of Tunnel  
After 10-atm Test

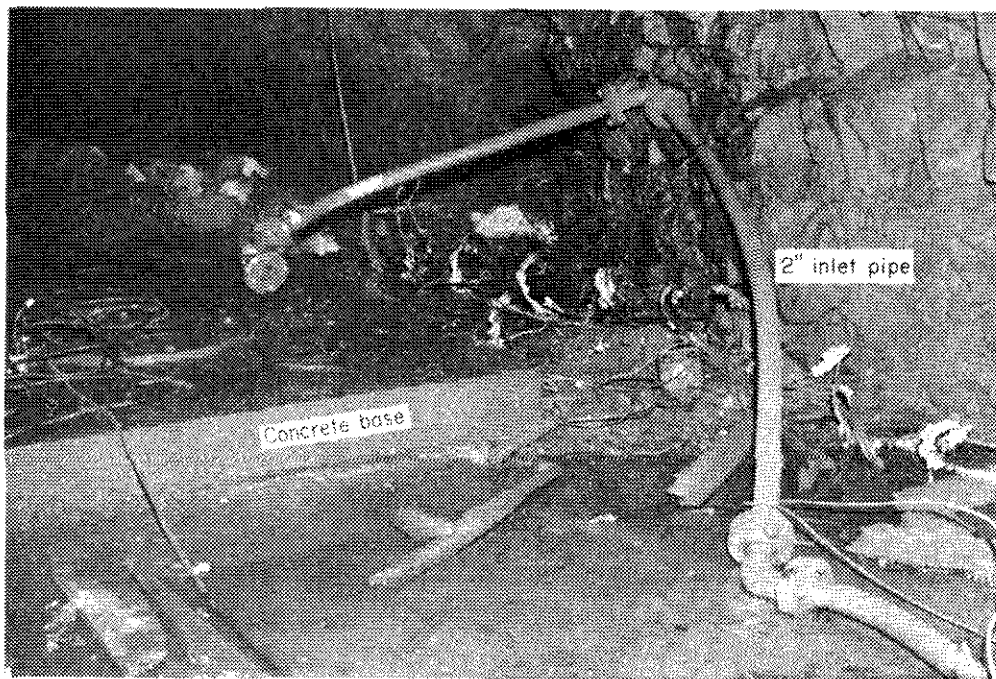


FIGURE 13. Concrete Base of Tank After 10-atm Test

pressure of 35 psi. It withstood over 150-psi static pressure during charging for Test 9 and 1085 psia dynamic pressure during Test 8. Although the diameter increased almost 1 ft during Test 8, no leak occurred. Following the first test, and each subsequent test, the tank's strength was progressively increased by cold-working, and the tank was capable of withstanding greater internal pressures than it had been originally designed for. If a new tank had been tested each time, rupture might have occurred at a somewhat lower test pressure. However, because only minimal yielding occurred during Tests 1 through 6 with test pressures  $\leq 3.1$  atm abs, the tank's strength had probably not been significantly increased above that of the original tank, and the original tank could have probably withstood deflagrations while operating at pressures  $\leq 3.1$  atm abs.

#### FLAME ARRESTER TESTS

A Kemp Manufacturing Company Model F22-C flame arrester was tested at two locations in a  $\frac{1}{2}$ -inch pipe. Figures 1e and 14 show the equipment diagrams and Figure 14 also shows arrester design and operating data. The F22-C model was chosen because it is widely used for flame protection in small lines, compatible with Savannah River processes ( $\sim 5\frac{1}{2}$  inches long). Introduction of any new equipment into the process hoods is difficult because of a limited amount of space, but this size arrester could be used to isolate ignition sources within process equipment.

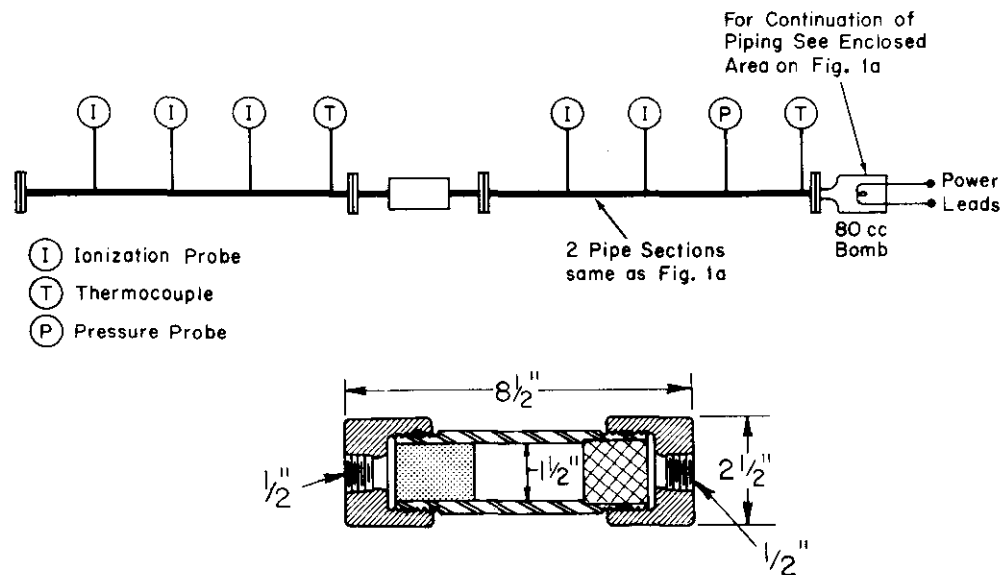


FIGURE 14. Flame Arrester Test Equipment Diagram

In all tests (Table I), the arrester failed to stop or slow the reaction front. This was expected in Tests 24 and 25 because the arrester was located at a point in the system where the reaction had reached the detonation stage, and literature data<sup>7</sup> on various commercial arresters indicated they reliably stopped detonations only where flame speeds were <350 ft/sec. In Tests 24 and 25, flame speeds at this point were in excess of 4500 ft/sec. In Tests 27 through 35, with the arrester located 16 inches from the ignition source and in the area of minimum reaction velocity, the arrester had been expected to stop the flame front. However, in these tests, the arrester also failed to stop or slow the flame front. The reaction velocity must have exceeded 350 ft/sec before reaching the arrester. Because it could not be placed nearer to the ignition source, the Kemp arrester was not suitable for use at Savannah River.

Discussions with flame arrester manufacturers revealed that none produce a standard arrester recommended for use in lines carrying hydrogen. Experimental types of arresting equipment in use with highly explosive gases were also found unsuitable for Savannah River processes.

## ACKNOWLEDGMENTS

All tests were conducted at Carney's Point Development Laboratory by T. P. Garrett, Jr., who developed deflagration-detonation data. Technical assistance was also provided by:

J. G. Brewer, Senior Design Consultant, who assisted in preparation of test outline and interpretation of results.

R. B. Brown, ESD Consultant, who assisted in conduct of tank tests, made strain measurements, assisted in interpretation of results, and issued study report on strain measurements.

R. P. Delano, Senior Design Consultant, who assisted in preparation of test outline and interpretation of results.

J. H. Faupel, Senior Design Consultant, who assisted in preparation of test outline, performed tank stress analysis calculations, and assisted in interpretation of results.

R. J. Landrum, ESD Senior Consultant, who conducted a metallurgical examination of tank material following tests and issued a report of findings.

## APPENDIX

### Peak Pressure Calculations for Pipe Tests

To calculate peak pressures from flame front velocity, the following equation<sup>6</sup> is used:

$$P_{\max}/P_i = (1 + \mu^2) M_o^2 - \mu^2 \quad (1)$$

where

$$\mu^2 = \frac{\gamma - 1}{\gamma + 1}$$

$$\gamma = \frac{C_p}{C_v}; \quad \gamma_{\text{air}} = 1.40, \gamma_{\text{H}_2} = 1.41, \gamma_{\text{mix}} = 1.4$$

$C_p$  = heat capacity at constant pressure

$C_v$  = heat capacity at constant volume

$P_{\max}$  = peak pressure, psia

$P_i$  = initial pressure, psia

$M_o$  = machine number, dimensionless =  $D/a$

$D$  = shock front velocity measured by probes, ft/sec

$$a = \text{sonic velocity in mixture, ft/sec} = \sqrt{\frac{\gamma RTg_c}{M}}$$

$g_c$  = conversion factor = 32.2 ft/sec<sup>2</sup>-lb

$T$  = absolute temperature, °R

$M$  = molecular weight of mixture;  $M_{\text{air}} = 28.97$ ,  $M_{\text{H}_2} = 2.016$ ,  
 $M_{\text{mix}} = 0.6 M_{\text{air}} + 0.4 M_{\text{H}_2} = 18.19$

$R$  = universal gas constant = 1545.33 ft-lb/°R-mole

$$a = 75 \left( \frac{\gamma R T g_c}{M} \right)^{1/2} = \left( \frac{1.4 \times 1545.33 \times 535 \times 32.2}{18.19} \right)^{1/2} = 1432 \text{ ft/sec}$$

The use of Equation 1 is illustrated with the data from Test 1, in which the propagation velocity was 5870 ft/sec.

$$M_o = D/a = 5870/1432 = 4.099$$

$$P_{\max}/P_i = \left( 1.0 + \frac{1.4 - 1.0}{1.4 + 1.0} \right) (4.099)^2 - \frac{1.4 - 1.0}{1.4 + 1.0} = 19.44$$

$$P_{\max} = 19.44 \widehat{P}_i = (19.44)(29.7) = 580 \text{ psia}$$



## REFERENCES

1. H. F. Coward and G. W. Jones. *Limits of Flammability of Gases and Vapors*. Bulletin 503, Bureau of Mines, U. S. Government Printing Office, Washington, D. C. (1952).
2. "Combustion." *Encyclopedia Britannica*, Vol VI, p. 98-99 (1958).
3. M. G. Zabetakis. *Flammability Characteristics of Combustible Gases and Vapors*. Bulletin 627, Bureau of Mines, U. S. Government Printing Office, Washington, D. C. (1965).
4. E. W. Cousins and P. E. Cotton. *Protection of Closed Vessels Against Internal Explosions*. Bulletin 741, National Fire Protection Association, Boston, Mass. (1951).
5. B. Lewis. *Combustion, Flames and Explosions of Gases*, 1st Ed., Macmillan, New York (1938).
6. J. F. Lee. *Thermodynamics*. 2nd Ed., Reading, Addison-Wesley, Cambridge, Mass. (1963).
7. P. A. Cubbage. In *Second Symposium on Chemical Process Hazards*, p. 31, Institution of Chemical Engineers, London (1963).

TML:sce

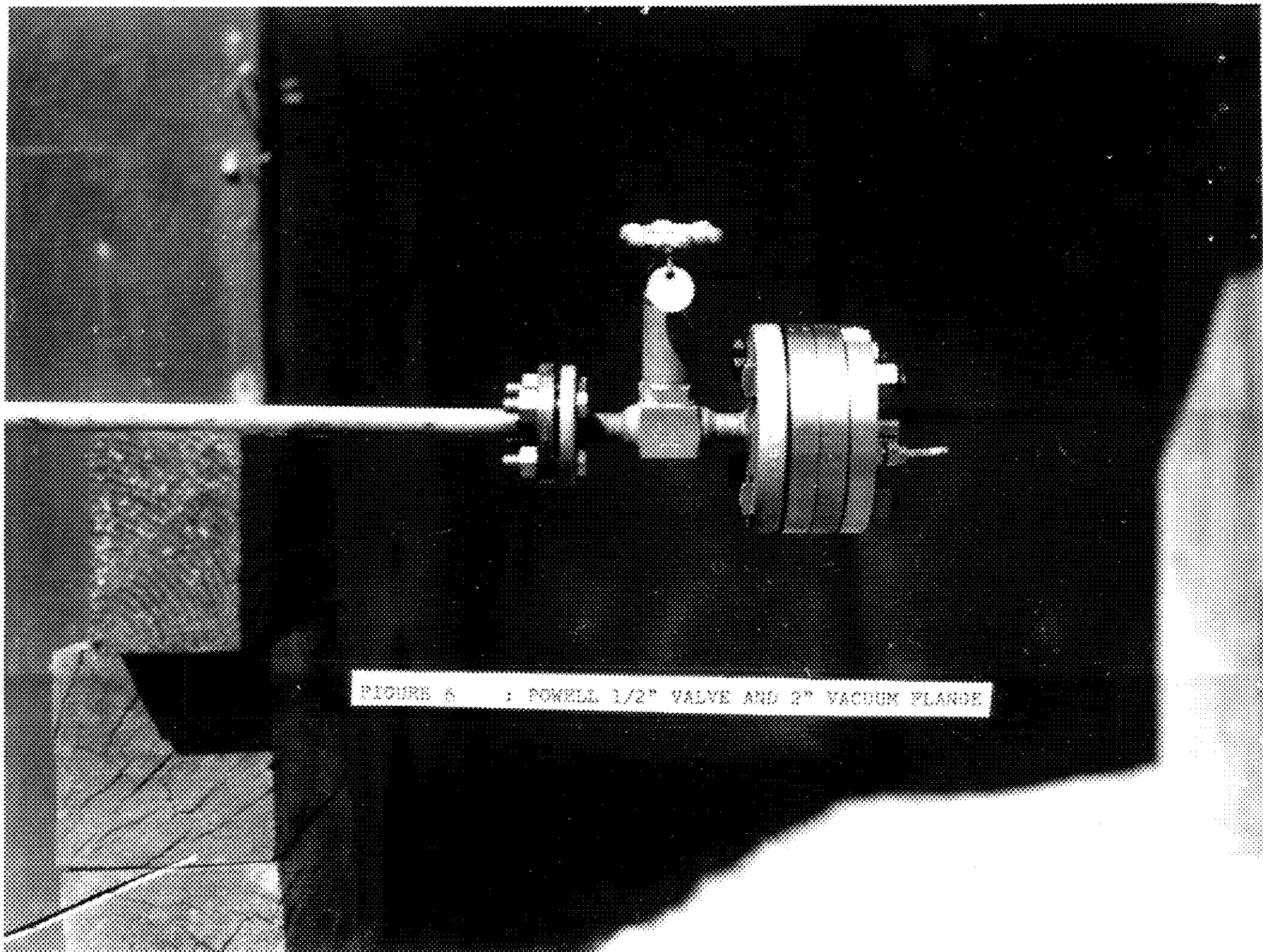


FIGURE 6 : POWELL 1/2" VALVE AND 2" VACUUM FLANGE



FIGURE 21 : TANK SECTION AFTER 10 ATM. TEST (FOUND  
35 FEET FROM ORIGINAL TANK LOCATION)

